Journal of Renewable Materials

Tech Science Press

Hygrothermal/UV Aging Effect on Visual Aspect and Mechanical Properties of Non-Woven Natural-Fiber Composites

Daniel Scida[1,*], Sébastien Alix[1], Stéphane Buet[1], El Hadi Saidane[1], François Courmont[1,2], Karim Behlouli[2] and Rezak Ayad[1]

[1]Université de Reims Champagne Ardenne, LISM EA4695, 51097 Reims, France.

[2]EcoTechnilin SAS, ZA Caux Multipôles 76190 Valliquerville, Arrondissement de Rouen, France.

[*]Corresponding Author: Daniel Scida. Email: daniel.scida@univ-reims.fr.

Abstract: This work aims at studying the effect of hygrothermal and UV cyclic aging on the tensile properties and esthetic characteristics of non-woven composites. The composite materials were thermo-compressed from non-woven mats made up of PP and flax or kenaf fibers. This works included evaluating the change in color appearance and analyzing the variations in tensile properties and damage mechanisms, depending on the aging time. The presence of the UV protection film on the composite surface showed its effectiveness against aging. From visual observations and measurement of colorimetric parameters, it has been proved effective in the reduction of the bleaching and yellowing of the composites. As regards the tensile tests, the UV protection film enabled to stabilize the Young's modulus after 1-week aging for Kenaf/PP and after 3-weeks for Flax/PP. After 4-weeks aging, it halved the number of acoustic emission events related to interfacial decohesion and fiber slippage/pull out for Flax/PP and Kenaf/PP composites.

Keywords: Aging; colorimetry; mechanical properties; natural fibers; non-woven

1 Introduction

Among composite materials based on renewable resources, non-woven biocomposites are becoming more and more attractive for the automotive industry. This increased attractiveness lies in their ability to combine acoustic absorption, lightweight, mechanical performance and acceptable processing time [1]. Natural-fiber and polypropylene (PP) composites in particular are increasingly used mainly to equip vehicle interior parts. These biocomposites are most frequently commingled (mixing natural fibers and PP), non-woven, manufactured and shaped by compression molding. They allow complex parts to be manufactured without performing the reinforcement prior to molding. It is simply necessary to produce upstream non-woven mats through a carding/cross-lapping/needle-punching process, reducing manufacturing costs compared to woven composites for example. Non-woven composites based on natural fibers such as flax, hemp, jute, kenaf, have the advantage of combining interesting mechanical and acoustic properties, which can be achieved by the control of their porosity ratio through the compression rate [2]. Indeed, they have acoustic absorption properties that can be used as noise-reducing components in automobiles [3]. The current trend is to remove the aesthetic coatings used today to keep a natural appearance by letting appear natural fibers. This raises the problem of their behavior over time in a sometimes aggressive environment. The lack of knowledge about durability is one of the main barriers to the development of the use of natural fibers-based reinforcement for composite applications. The exposure to moisture, ultra-violet (UV) radiation and temperature, and mainly a combination of these aging processes may degrade the properties of natural-fiber reinforced PP composites. Several studies investigated the influence of these aging types on their mechanical and visual aspect properties [4-14]. In a work of Yan et al. [4], the combined effect of UV radiation and water spraying UV caused color fading and loss in stiffness and strength of flax/epoxy composites. Several works by a Brazilian team [5-7] have

studied the effect of aging (UV, water condensation and temperature) on PP and high-density polyethylene (HDPE) matrices reinforced with cellulosic fibers by demonstrating the impact of the lignin content of the fibers. Lignin, which has an antioxidant role, increases the stability of biocomposites in the face of aging. According to Peng et al. [10], the color fading of wood flour (WF) and PP composites was attributed to photodegradation or photobleaching of lignin in the WF. The photo-oxidation of lignin could cause discoloration of samples altered by accelerated weathering. This color change became more significant with the increasing of natural-fiber content in the composite, as shown a study of Butylina et al. [12]. Badji et al. [14] studied the influence of weathering on visual and surface aspect of wood plastic composites. Analyses of surface microstructure and colorimetry revealed that aging induced a surface bleaching, a wood particle protrusion and numerous microcracks.

The degradation mechanisms of PP promoted by UV-accelerated aging also have an impact on the properties of aged biocomposites. Beg and Pickering [15] studied the aging (moisture/UV) of PP matrices and specified that the photodegradation of PP was mainly due to photo-oxidation, particularly concentrated near the surface and in the amorphous parts of the polymer which are more permeable. The color of the matrix has a great importance on the aging of composites. Many studies on the subject have shown the impact of pigments on the color change of the parts produced. For example, Du et al. [16] studied the effects of different color pigments on the durability of WF/HDPE composites evaluated by UV-accelerated weathering tests. All samples showed significant fading and color changes in exposed areas. In particular, the addition of carbon black had the greatest protective effect among all the pigments, showing the least fading. The authors suggested the black pigment might shield more UV-light or screen from composite lightening than the other color pigments. Pigments can protect the matrix of WF/HDPE composites from UV degradation to a certain extent, and carbon black was more effective than the other pigments. However, pigment did not prevent lignin degradation in the WF/HDPE composites since lignin is very sensitive to UV light. Note that Butylina et al. [12] have found similar results on PP/wood biocomposites: increased aging stability with dark pigments (grey and brown) and influence of lignin on chemical changes caused by UV radiation.

Despite these works on weathering of natural-fiber composites, most of it focused on WF composites. In addition, few works to the best of our knowledge addressed an in-depth analysis of the damage mechanisms caused both by cyclic aging due to UV radiation and water condensation and by tensile loading. This is why this study focused on an aging combined with UV, water condensation and temperature of plant-fiber composites. The aim was to study the effect of hygrothermal and UV cyclic aging on the esthetic characteristics, the tensile properties and the damage mechanisms of non-woven composites. The composites were manufactured by thermo-compression from non-woven mats made up of PP and flax or kenaf fibers. The tensile tests were monitored using the acoustic emission (AE) technique to identify the different damage mechanisms of these unaged or aged composites. This was conducted using an unsupervised method based on multivariable statistical analysis. This works included evaluating the change in color appearance and analyzing the changes in tensile properties and damage mechanisms, depending on the aging time. The presence or no of an UV protection film on the composite surface was particularly investigated.

2 Materials and Methods

2.1 Materials and Manufacturing Process

Two different non-woven composites, named Flax/PP and Kenaf/PP, were performed by combining black PP with flax fibers and natural PP (without coloring) with kenaf fibers, respectively. All fibers, 8-10 mm long, were chosen because they were widely used in automotive industry [17]. The black PP was composed of natural PP to which 0.5% of carbon black was added. Industrial commingled non-wovens were manufactured by EcoTechnilin® SAS (Valliquerville, France) at a fiber matrix ratio of 50%-wt according to the carding/over-lapping/needle punching technology [18]. The non-woven composites, whose specifications are reported in Tab. 1, were thermo-compressed from 5 plies of 300 g/m² non-woven, with same processing parameters. During thermo-compression manufacturing of composite, a transparent

UV protection film (180 g/m² weight and ≈ 60 μm thick) was added or no on the upper side of the 5-ply multilayer (defined by wF: without Film or F: with Film).

Table 1: Weight, thickness and fiber volume content of non-woven composites

Composite designation	Presence of UV protection film	Areal weight (g/m²)	Thickness (mm)	Fiber content v_f (Vol.%)
Flax/PP-wF	No	1500	1.48 ± 0.05	38.3
Flax/PP-F	Yes	1500/180	1.54 ± 0.05	38.3
Kenaf/PP-wF	No	1500	1.56 ± 0.07	42.3
Kenaf/PP-F	Yes	1500/180	1.62 ± 0.03	42.3

2.2 Aging Tests

The artificial aging was conducted in a QUV test chamber (Q-Lab Corporation, Westlake, Ohio, USA) equipped with UVB-313 lamps (280-315 nm) in order to simulate degradations caused by sunlight, rain and water condensation [19]. Each cycle consists of 4h condensation (relative humidity close to 100%) at 50°C without UV and then 8h UV exposure at 70°C without condensation. This cycle was chosen to continuously age test pieces in an aggressive environment, according to cycle 6 of ISO 4892-3 standard [20].

2.3 Colorimetric Tests

For different aging periods (from 0 to 4 weeks), the colorimetric parameters were measured with a Minolta CR300 chroma meter, from the 3 coordinates L^*, a^*, b^* of the CieLab color space, generating a quantitative description of color, as described in [21]. The luminance L^* is characteristic of the relative brightness from total black (0) to pure white (100). The parameter a^* give the range from red (-100) to green (+ 100) and b^* from blue (-100) to yellow (+ 100). $\Delta L^* = L_t^* - L_0^*$, $\Delta a^* = a_t^* - a_0^*$ and $\Delta b^* = b_t^* - b_0^*$ (L_t^*, a_t^* and b_t^* are the coordinates of the specimen aged for a time t and L_0^*, a_0^* and b_0^* the coordinates of unaged specimen) are calculated to assess the evolution between the initial state and the state after cyclic aging. The total color difference (ΔE^*) between the aged and unaged specimen were obtained using the relation $\Delta E^* = [(\Delta L^*)^2 + (\Delta a^*)^2 + (\Delta b^*)^2]^{1/2}$, in CieLab units. The instrument was calibrated using a standard white plate provided by the manufacturer, before measurements at the specimen center were done.

2.4 Tensile Tests

The tensile tests were conducted on an Instron 3382 universal machine, following the ISO 527-4 standard [22]. The width and length of the specimen were 25 and 250 mm, respectively. All tests were performed at room temperature with a 2 mm/min crosshead speed and a 5 kN static load cell. To ensure that breaks would occur in the middle of the specimen, glass/epoxy composite tabs were bonded at the ends of each specimen. Axial clip-on extensometer was used to measure the longitudinal strains, with a measurement range of 25 mm. For each composite, five tests were carried out. The average value and the standard deviation were then reported.

2.5 Acoustic Emission

AE was continuously monitored during the tensile tests to obtain information about damage

evolution. AE measurements were conducted using two channels data acquisition system (Mistras Group), with sampling rate 5 MHz and a 40 dB pre-amplification. AE signals were achieved by two resonant Micro-80 piezoelectric sensors with a frequency range of 100 kHz-1 MHz and a resonance peak of around 300 kHz. The sensors were placed on the surface of the tensile specimen at both ends and a spacing of 87 mm. To provide a good acoustic coupling, a silicone grease was employed as a coupling agent between the sensors and the sample surface. The AE signals obtained during tensile tests on the studied specimens were analyzed by considering a statistical multi-variable analysis using Noesis Software, as detailed in [23].

3 Results and Discussion

3.1 Colorimetric Parameters

Fig. 1 shows the change in appearance of the two non-filmed composites without aging and after 1, 2, 3 and 4-weeks aging. One can note that colors are darker on Flax/PP-wF than Kenaf/PP-wF, due to the matrix color (black for Flax/PP and natural for Kenaf/PP). The more the aging time increases, the more the flax fibers become increasingly visible. In addition, the black color of the PP matrix lightens and becomes gray or white near the apparent fibers on the surface. The color of Kenaf/PP-wF lightens in the first two aging weeks reaching light beige and darks in the next two aging weeks reaching deep beige. Note that the kenaf fibers are more visible and deposition of white chalky material is observed on the surface of both non-filmed composites after aging. This is found in larger quantity as the aging time increases. These white powders must be produced during the degradation of the polymer due to the UV rays converting it as a powdery material on the surface. The PP degraded layer with a chalky appearance was reported in previous works on the degradability of polymeric composites based on natural fibers [8, 15]. The same phenomenon was detected, for example, in works on combined moisture/UV weathering of wood fiber reinforced PP composites [15].

From visual observations, the filmed samples practically do not change color with aging and do not show powders or flours on their surface. The presence of the UV protection film shows visually its effectiveness against the aging.

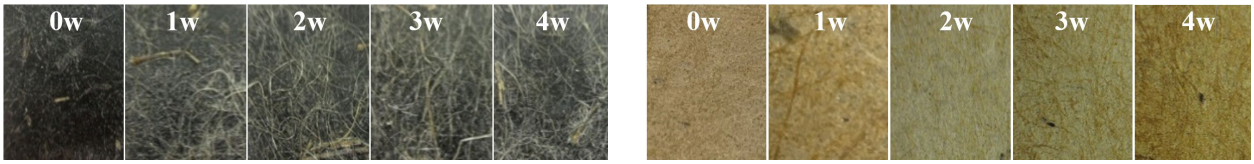

(a) (b)

Figure 1: Pictures of the specimen surfaces for aging periods from 0 to 4 weeks, for non-filmed Flax/PP (a) and non-filmed Kenaf/PP (b) composites

To quantitatively assess the color changes due to the aging, the colorimetric parameters were measured at the center of each specimen in the Cielab system [21], which has the properties of a Euclidean space. Indeed, the distance between two color points, one measured on the unaged specimen and the other on the aged specimen, represents their colorimetric difference (ΔE^*) and is calculated from the changes of its Cartesian components, ΔL^*, Δa^* and Δb^*. Fig. 2 shows the changes of the parameters L^*, a^*, b^* and E^* according to the aging times, from 0 to 4 weeks. The results show that these parameters of filmed and non-filmed Flax/PP follow the same evolution during aging. After 4-weeks aging, Flax/PP tend to be very slightly less red ($\Delta a^* \approx -2$) and more yellow ($\Delta b^* \approx 2$), and the UV protection film has almost no effect on these changes. In contrast, it reduces the impact of aging on the bleaching ($\Delta L^* \approx 4$ *vs.* 12 without film, after 4 weeks) and therefore on the color change E^* (-7 points). The changes in ΔE^* for all composites were closed to the changes in ΔL^*, as mentioned in former studies [10]. The finding is similar for Kenaf/PP since the film reduces L^* and E^* by 8 and 9 points respectively. Note that the Kenaf/PP photobleaching was faster than the Flax/PP one. This can be explained by two hypotheses: 1)

by the nature of the matrix, the black PP matrix containing carbon black absorbs UV radiation more easily at the wavelengths of the study and 2) by the chemical composition of fibers, in particular the cellulose and lignin contents (71 and 2.2 wt%, respectively for flax; 45-57 and 8-13 wt%, respectively for kenaf [24]). Indeed, lignin-based composites showed higher ΔL^* values than the cellulose-based composites one, suggesting that photobleaching of lignin was easier and faster than cellulose [10]. Furthermore, another difference with Flax/PP is in the evolution of Δb^* increasing by 7 points for the Kenaf/PP-wF after 4-weeks aging. Again, the sensitivity of lignin to light leads to photochemical reactions of lignin, which are responsible for most of the color change, in particular of the yellowing [12]. In conclusion, the presence of the UV protection film showed its effectiveness against the aging, both with visual observations and colorimetric parameters. It has been proved effective in the reduction of the bleaching and yellowing of the composites.

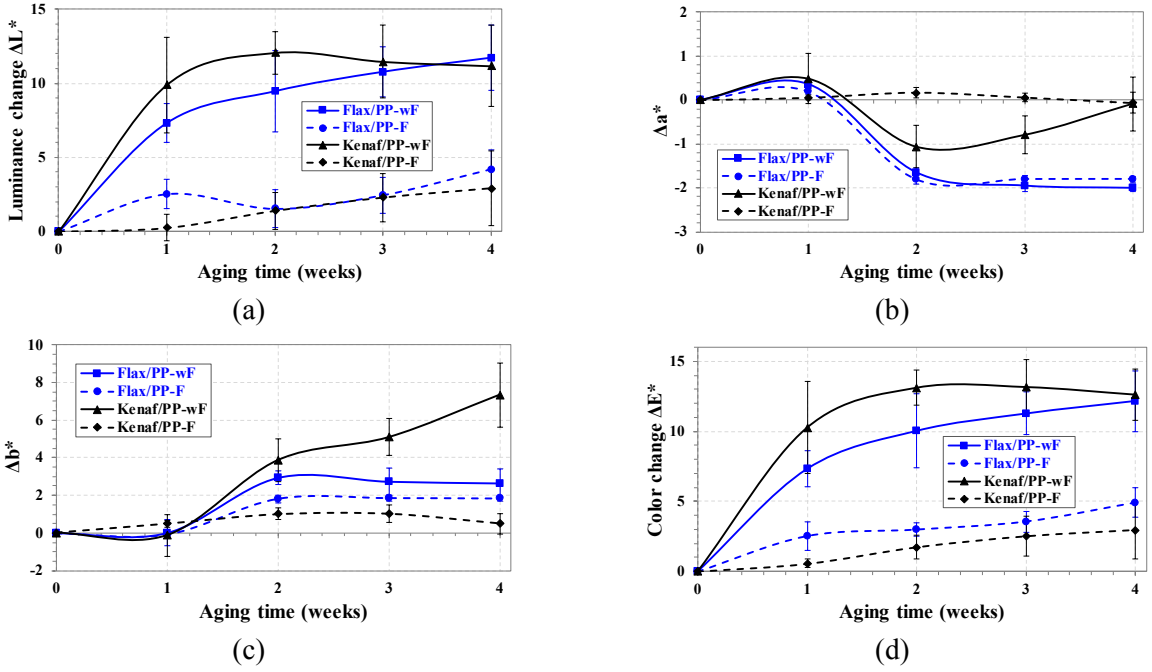

Figure 2: Changes of (a) luminance L^*, (b) parameter a^*, (c) parameter b^* and (d) color E^* of the composites, as a function of aging times

3.2 Mechanical Behavior

3.2.1 Influence of the Tensile Direction

Initial tensile tests were performed in both perpendicular directions of the non-woven plate, first in the Machine Direction (MD) and second in the Cross-machine Direction (CD). Fig. 3 reports results of Young's modulus and tensile strength for the unaged composites. One can notice that values of Young's modulus in the CD are higher than those in the MD, for both non-filmed and filmed composites. This difference in both directions is related to the anisotropy of the non-woven in its dry form, as shown a recent study of Gnaba et al. [25]. This is mainly due to the manufacturing process which orientates the fibers in the CD and to the anisotropy of the kenaf and flax fibers [26,27]. This difference is also noted for the tensile strength of Kenaf/PP and it is not as pronounced for Flax/PP. The fiber morphology (straight, ramified…) has certainly important impacts on the capacity of the carding machine to orientate the fibers. Thereafter, only results in the CD are reported in the next sections.

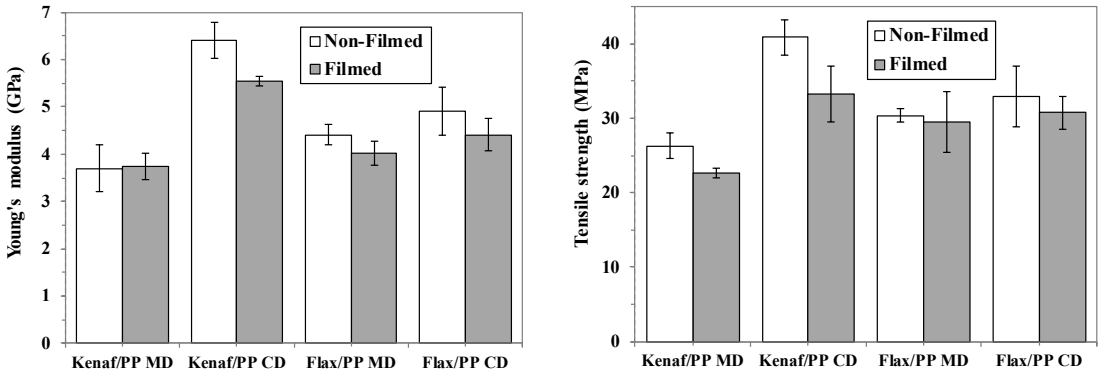

Figure 3: Young's modulus (a) and tensile strength (b) of the unaged composites, in the MD and CD

3.2.2 Influence of UV Aging

Initial aging tests mainly focused on UV aging and the Flax/PP-wF was exposed to 265 h of UV light at 70°C. Results show that the Young's modulus increase (+ 22%) whereas the tensile strength varies only slightly (+ 4%). The stiffening of the composite is explained by changes in the polymer matrix due to UV radiation. In the first few hundred hours of exposure, chain scission in the PP matrix occurs, and shorter chains have higher mobility, making it easier to reorganize. It results in an increase in crystallinity and thus in modulus, as explained in previous works [11,28].

3.2.3 Influence of Hygrothermal and UV Cyclic Aging

Figs. 4 and 5 present the values of Young's modulus and tensile strength, at different aging times (1, 2, 3 and 4-weeks aging). The UV protection film slightly reduces the both properties for the unaged composites but reduces the impact of aging. From 2-weeks aging, the modulus of the filmed samples become superior to the modulus of the non-filmed samples and more significantly for Kenaf/PP. The film associated with a lower porosity ratio is particularly effective over time for Kenaf/PP. After a decrease in modulus, this one is stabilizing after the 1st-week aging. For the Flax/PP-F, the modulus stabilizes only after 3-weeks aging but is more degraded by the aging. This difference between Flax/PP and Kenaf/PP can be attributed to 1) the influence of the matrix color and 2) the high hydrophilicity of the chemical compositions of both flax and kenaf fibers. Indeed, the UV light and water spraying cycles had negative effect on the main contents of plant fiber, in particular cellulose and hemicellulose [4]. The cumulative content of cellulose and hemicellulose for flax and kenaf fibers can be up to 89.6-91.6% and 66.5-78.5%, respectively, which might explain the different degradation in modulus. Note that, whatever the composite, the loss in Young's modulus is more pronounced after the 1st-week aging, with reduction from 25 to 44%. As regards the tensile strength, the loss due to aging is less pronounced, except for the Kenaf/PP-wF. Values are close to 29.5 ± 1 MPa after 4-weeks aging whatever the composite, which corresponds approximatively to the tensile strength of neat PP.

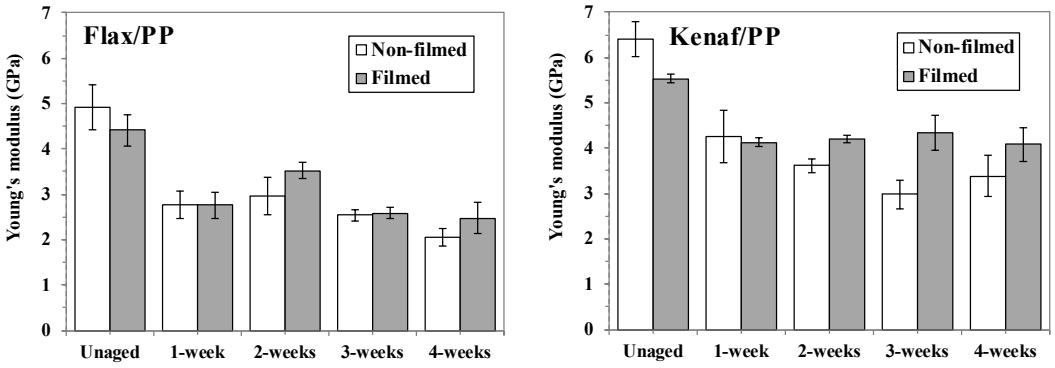

(a) (b)

Figure 4: Young's modulus versus aging times for Flax/PP (a) and Kenaf/PP (b) composites

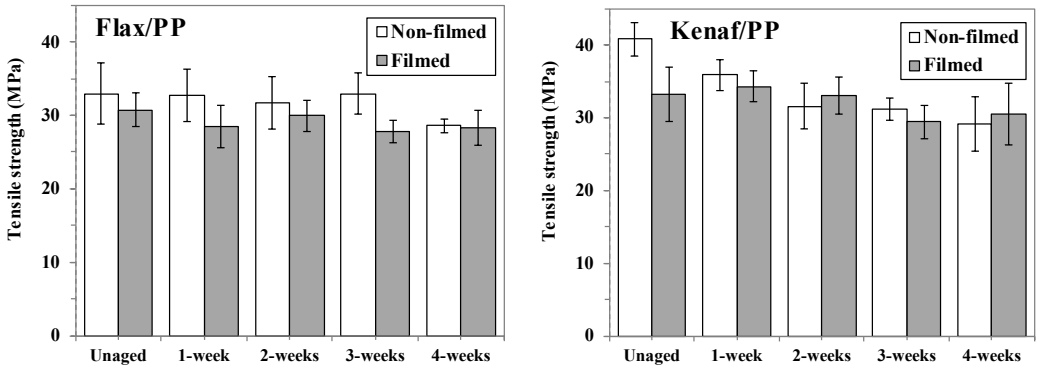

(a) (b)

Figure 5: Tensile strength versus aging times for Flax/PP (a) and Kenaf/PP (b) composites

3.3 Analysis of Damage Mechanisms

A multi-variable statistical analysis to classify acoustic emission signals described in detail in [23] had identified three classes of AE signals for all studied composites. The characteristics of the recorded AE signals were compared with the literature results in order to associate the three obtained classes with their corresponding damage mechanisms. Fig. 6 presents the amplitude ranges of AE signals according to the three classes for unaged and 4-weeks aged composites. The borders of box plots of the three AE classes indicate the first quartile q_1 and the third quartile q_3. The lines cutting through the box plots present the median (the second quartile q_2). The whisker corresponds to the lower and upper values of the amplitude range of each class. It was shown that the AE signals of the first class were characterized by low amplitudes centered around 40 dB and very low energy level. They were associated with the matrix cracking mechanisms. The same characteristics, well known in the literature, were obtained for flax/Elium [29], hemp/PP [30] and flax/LPET composites [31], among others. The AE signals of the second class were more energetic and identified at an amplitude between 45 and 65 dB for unaged and aged materials. This amplitude range was attributed to the fiber-matrix debonding mechanism in accordance with the literature [29-32]. The higher amplitudes made it possible to identify the last class. It was detected at the 75-90 dB amplitude range, except for the aged non-filmed composites (65-80 dB). The corresponding AE signals were characteristic of damage mechanisms that typically appeared in non-woven natural-fiber composites close to their tensile failure. These were only caused by the fiber, such as fiber slippage and pull out of the elementary fibers in the bundle [31]. Note that the fiber bundle breakage was considered in the range of 80-100 dB associated with a high energy level [31]. This signal type was atypical of our last class. Only 4-7% of the signals were detected with amplitudes over 80 dB for the

flax/PP composites for example. The amplitude offset for the aged non-filmed composites could be attributed to the degradation of flax and kenaf fibers caused by the hygrothermal and UV cyclic aging. It is worth noting that the UV protection film played its role in protecting both materials against aging because the amplitude range was not affected.

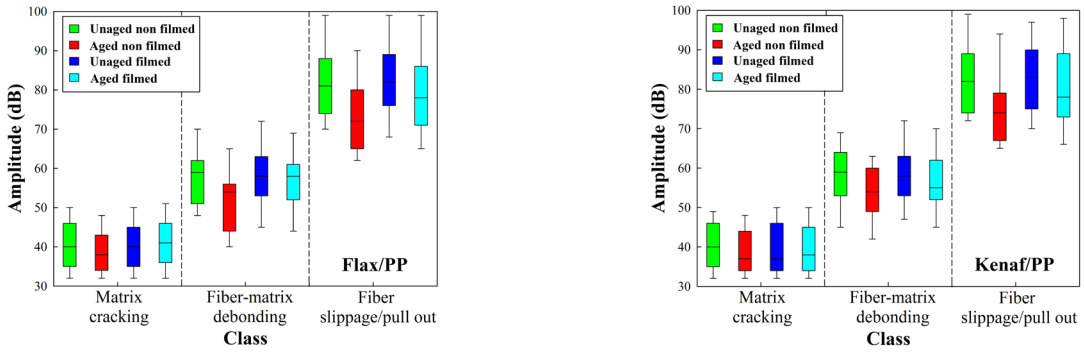

Figure 6: Amplitude ranges of AE signals versus the three damage mechanisms for Flax/PP (a) and Kenaf/PP (b) composites

To illustrate the damage mechanisms during tensile tests, the evolution versus time and strain of the cumulative hit number of each class, combined with tensile strength was analyzed. One of the results is shown in Fig. 7. The results show that the acoustic activity starts in a progressive way between the first third and half of the tensile test duration, and then it grows exponentially close to the end of the tensile test until the specimen failure. The acoustic activity starts from 3% of the strain at failure for unaged composites and almost from the beginning of the tensile test for aged composites. For all composites, the matrix cracking signals were the first detected. Then, the AE signals induced by the fiber-matrix debonding really started at the middle stage of the test, in the strain range of 0.9-1.1% and its number growed with the increase of tensile strength and tensile strain. The signals associated with the fiber slippage and pull out intensified exponentially when getting closer of the strength at failure of the material. Indeed, three quarters of the AE events of this class appeared in the last three twentieths of the test duration. In addition, the AE classification showed that the matrix cracking presented more than 65% of cumulative hit number for unaged and aged composites.

The obtained results also indicate a decrease in the cumulative hit number induced by the matrix cracking for aged non-filmed composite with respect to unaged one, by about 25%. For the aged filmed composite, a decrease of less than 10% was observed. In addition, the UV protection film played a significant role in protecting both materials against aging, reducing by half the number of events related to interfacial decohesion and fiber slippage/pull out. This was not observed for the aged non-filmed composite.

In order to assess the contribution of each damage mechanism to the composite failure, the cumulative AE energy was used to analyze the signals. The Damage Contribution (DC) was defined by the cumulative AE energy of each mode divided by the total cumulative energy [23]. Fig. 8 reports the relative DC of each damage mode for unaged and 4-weeks aged materials. It showed that the most significant DC was the fiber-matrix debonding (> 50%). Indeed, the composite failure was mostly caused by the fiber-matrix debonding due to the imperfect bonding [2]. This result indicated that the fiber-matrix interface played a significant role in the damage of non-woven composites. For all materials, the second most damaging mode was the fiber slippage/pull out (26-47%). After the interfacial bond failure, fibers were pulled out from the matrix [2]. In addition, at the fracture surface, elementary fibers were slipped and debonded inside the bundle. The third damage mode was the matrix cracking which was low in energy (< 5%). After 4-weeks aging, the DC of the fiber-matrix debonding was slightly increased by about 10 and 6% for the Flax/PP-wF and Kenaf/PP-wF composites, respectively. This increase was accompanied by a decrease in the fiber slippage/pull out DC of both aged composites (10% and 4%,

respectively). These phenomena were mainly due to the fiber swelling and the degradation of the flax and kenaf fibers caused by the hygrothermal aging, particularly by the water absorption [33]. For the filmed composites, these changes with aging were lower. The DC of the fiber-matrix debonding remained stable after 4-weeks aging. Concerning the DC of the fiber slippage/pull out, a decrease of less than 5% and 2% was observed for the aged Flax/PP-F and Kenaf/PP-F composites, respectively. This result highlighted that the incorporation of the UV protection film offered good protection against the studied aging as well as an improvement in durability of composites.

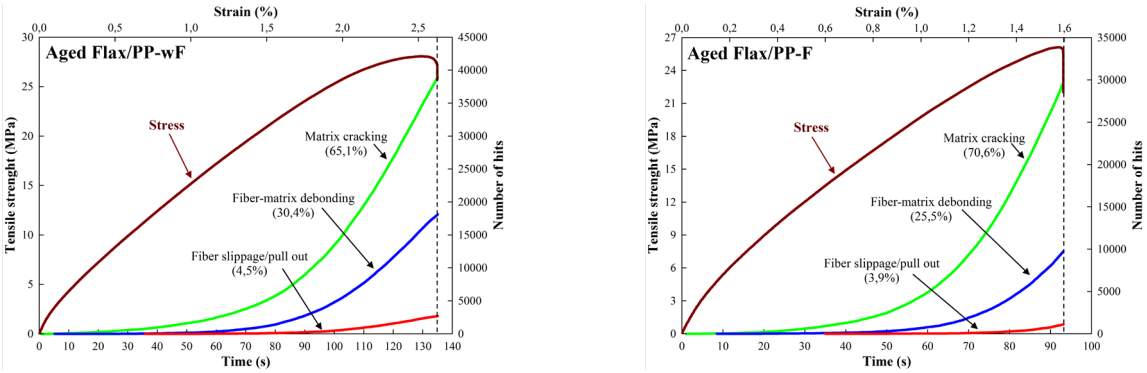

(a) (b)

Figure 7: Tensile strength and number of hits versus tensile tests strain and time for aged Flax/PP, non-filmed (a) and filmed (b)

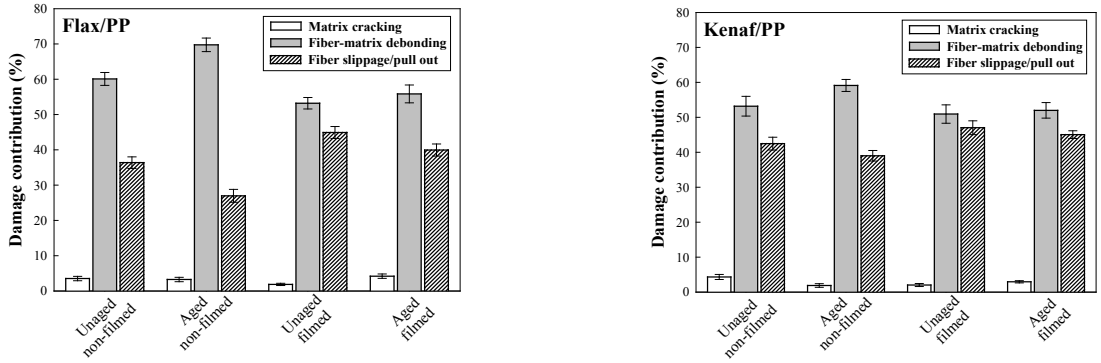

(a) (b)

Figure 8: Damage contribution for Flax/PP (a) and Kenaf/PP (b) composites

4 Conclusions

This work aimed at studying the effect of hygrothermal and UV cyclic aging on the tensile properties and esthetic characteristics of non-woven composites, composed of PP and flax or kenaf fibers. The composites were subjected to repetitive cycles of aging (4 h condensation at 50°C + 8 h UV exposure at 70°C). From the aging time, the change in color appearance was evaluated and the variations in tensile properties and damage mechanisms were analyzed. The presence of the UV protection film showed its effectiveness against aging, both with visual observations and analysis of colorimetric parameters. It has been proved effective in the reduction of the bleaching and yellowing of the composites. Without this protection, cyclic aging mainly affected the bleaching of both composites. Kenaf/PP bleached faster than Flax/PP, which can be explained by 1) the black color of the matrix and 2) their chemical composition in cellulose and lignin. In addition, higher yellowing was noted for Kenaf/PP because of its lignin content. As regards the tensile tests, the film enabled to stabilize the Young's modulus after 1-week aging for Kenaf/PP and after 3-weeks for Flax/PP. After 4-weeks aging, it halved the number of acoustic emission

events related to interfacial decohesion and fiber slippage/pull out for both composites and the amplitude ranges of the three detected damage modes was not affected.

Acknowledgement: The authors would like to gratefully thank the company EcoTechnilin for funding this study. Note that E.H. Saidane is a teacher-researcher since oct. 2017 at UHA in LPMT research lab.

References

1. Dunne, R., Desai, D., Sadiku, R., Jayaramudu J. (2016). A review of natural fibres, their sustainability and automotive applications. *Journal of Reinforced Plastics and Composites, 35(13),* 1041-1050.
2. Merotte, J., Le Duigou, A., Bourmaud, A., Behlouli, K., Baley, C. (2016). Mechanical and acoustic behaviour of porosity controlled randomly dispersed flax/PP biocomposite. *Polymer Testing, 51,* 174-180.
3. Parikh, D. V., Chen, Y., Sun, L. (2006). Reducing automotive interior noise with natural fiber nonwoven floor covering systems. *Textile Research Journal, 76(11),* 813-820.
4. Yan, L., Chouw, N., Jayaraman, K. (2015). Effect of UV and water spraying on the mechanical properties of flax fabric reinforced polymer composites used for civil engineering applications. *Materials & Design, 71,* 17-25.
5. Gadioli, R., Morais, J. A., Waldman, W. R., De Paoli, M. A. (2014). The role of lignin in polypropylene composites with semi-bleached cellulose fibers: mechanical properties and its activity as antioxidant. *Polymer Degradation and Stability, 108,* 23-34.
6. Guilhen, A., Gadioli, R., Fernandes, F. C., Waldman, W. R., Aurelio De Paoli, M. (2017). High‐density green polyethylene biocomposite reinforced with cellulose fibers and using lignin as antioxidant. *Journal of Applied Polymer Science, 134(35),* 45219.
7. Gadioli, R., Waldman, W. R., De Paoli, M. A. (2016). Lignin as a green primary antioxidant for polypropylene. *Journal of Applied Polymer Science, 133(45),* 43558.
8. Azwa, Z. N., Yousif, B. F., Manalo, A. C., Karunasena, W. (2013). A review on the degradability of polymeric composites based on natural fibres. *Materials & Design, 47,* 424-442.
9. Moriana, R., Strömberg, E., Ribes, A., Karlsson, S. (2014). Degradation behaviour of natural fibre reinforced starch-based composites under different environmental conditions. *Journal of Renewable Materials, 2(2),* 145-156.
10. Peng, Y., Liu, R., Cao, J., Chen, Y. (2014). Effects of UV weathering on surface properties of polypropylene composites reinforced with wood flour, lignin, and cellulose. *Applied Surface Science, 317,* 385-392.
11. Soccalingame, L., Perrin, D., Bénézet, J. C., Mani, S., Coiffier, F. et al. (2015). Reprocessing of artificial UV-weathered wood flour reinforced polypropylene composites. *Polymer Degradation and Stability, 120,* 313-327.
12. Butylina, S., Hyvärinen, M., Kärki, T. (2012). A study of surface changes of wood-polypropylene composites as the result of exterior weathering. *Polymer Degradation and Stability, 97(3),* 337-345.
13. Sauget, A., Zhou, X., Pizzi, A. (2014). Tannin-resorcinol-formaldehyde resin and flax fiber biocomposites. *Journal of Renewable Materials, 2(3),* 173-181.
14. Badji, C., Soccalingame, L., Garay, H., Bergeret, A., Bénézet, J. C. (2017). Influence of weathering on visual and surface aspect of wood plastic composites: correlation approach with mechanical properties and microstructure. *Polymer Degradation and Stability, 137,* 162-172.
15. Beg, M. D. H., Pickering, K. L. (2008). Accelerated weathering of unbleached and bleached kraft wood fibre reinforced polypropylene composites. *Polymer Degradation and Stability, 93(10),* 1939-1946.
16. Du, H., Wang, W., Wang, Q., Zhang, Z., Sui, S. et al. (2010). Effects of pigments on the UV degradation of wood‐flour/HDPE composites. *Journal of Applied Polymer Science, 118(2),* 1068-1076.
17. Carus, M., Eder, A., Dammer, L., Korte, H., Scholz, L. et al. (2015). Wood-Plastic Composites (WPC) and Natural Fibre Composites (NFC): European and global markets 2012 and future trends. *Nova-Institute: Hürth, Germany, 16.*
18. Russell, S. J. (2006). *Handbook of Nonwovens*. Location: woodhead Publishing, Cambridge, England.
19. Wypych, G. (1995). *Handbook of Material Weathering*. ChemTec Publishers, Toronto, Canada.
20. ISO 4892-3 (2016). Plastics-methods of exposure to laboratory light sources-Part 3: fluorescent UV lamps. *International Organization for Standardization*.

21. Dupont, D., Steen, D. (2004). Colorimétrie-Mesure des couleurs de surface. *Techniques de L'ingénieur. Mesures et Contrôle*, R6442.
22. ISO 527-4 (1997). Plastics-determination of tensile properties-Part 4: test conditions for isotropic and orthotropic fibre-reinforced plastic composites. *International Organization for Standardization*.
23. Saidane, E. H., Scida, D., Assarar, M., Ayad, R. (2017). Damage mechanisms assessment of hybrid flax-glass fibre composites using acoustic emission. *Composite Structures, 174,* 1-11.
24. Taj, S., Munawar, M. A., Khan, S. (2007). Natural fiber-reinforced polymer composites. *Proceedings-Pakistan Academy of Sciences, 44(2),* 129-144.
25. Gnaba, I., Omrani, F., Wang, P., Soulat, D., Ferreira, M. et al. (2019). Mechanical behavior of flax/polypropylene commingled nonwoven at dry scale: influence of process parameters. *Textile Research Journal, 89(5),* 791-800.
26. Andre, N. G., Ariawan, D., Mohd Ishak, Z. A. (2016). Elastic anisotropy of kenaf fibre and micromechanical modeling of nonwoven kenaf fibre/epoxy composites. *Journal of Reinforced Plastics and Composites, 35(19),* 1424-1433.
27. Baley, C., Perrot, Y., Busnel, F., Guezenoc, H., Davies, P. (2006). Transverse tensile behaviour of unidirectional plies reinforced with flax fibres. *Materials Letters, 60(24),* 2984-2987.
28. Stark, N. M., Matuana, L. M. (2003). Ultraviolet weathering of photostabilized wood-flour-filled high‐density polyethylene composites. *Journal of Applied Polymer Science, 90(10),* 2609-2617.
29. Monti, A., El Mahi, A., Jendli, Z., Guillaumat, L. (2016). Mechanical behaviour and damage mechanisms analysis of a flax-fibre reinforced composite by acoustic emission. *Composites Part A: Applied Science and Manufacturing, 90,* 100-110.
30. Assarar, M., Scida, D., Zouari, W., Saidane, E. H., Ayad, R. (2016). Acoustic emission characterization of damage in short hemp‐fiber‐reinforced polypropylene composites. *Polymer Composites, 37(4),* 1101-1112.
31. Aslan, M. (2013). Investigation of damage mechanism of flax fibre LPET commingled composites by acoustic emission. *Composites Part B: Engineering, 54,* 289-297.
32. Saidane, E. H., Scida, D., Pac, M. J., Ayad, R. (2019). Mode-I interlaminar fracture toughness of flax, glass and hybrid flax-glass fibre woven composites: failure mechanism evaluation using acoustic emission analysis. *Polymer Testing, 75,* 246-253.
33. Le Duigou, A., Merotte, J., Bourmaud, A., Davies, P., Belhouli, K. et al. (2017). Hygroscopic expansion: a key point to describe natural fibre/polymer matrix interface bond strength. *Composites Science and Technology, 151,* 228-233.